

****Volume Title****

*ASP Conference Series, Vol. **Volume Number***

****Author****

© ****Copyright Year**** *Astronomical Society of the Pacific*

Constraining Mass-Loss & Lifetimes of Low Mass, Low Metallicity AGB Stars

Philip Rosenfield¹, Paola Marigo¹, Léo Girardi², Julianne J. Dalcanton³, Alessandro Bressan⁴, Marco Gullieuszik², Daniel Weisz^{3,5}, Benjamin F. Williams³, Andrew Dolphin⁶, and Bernhard Aringer⁷

¹*Dept. of Physics and Astronomy G. Galilei, University of Padova, Vicolo dell'Osservatorio 3, I-35122 Padova, Italy*

²*Osservatorio Astronomico di Padova – INAF, Vicolo dell'Osservatorio 5, I-35122 Padova, Italy*

³*Dept. of Astronomy, University of Washington, Box 351580, Seattle, WA 98195, USA*

⁴*Astrophysics Sector, SISSA, Via Bonomea 265, I-34136 Trieste, Italy*

⁵*Hubble Fellow*

⁶*Raytheon Company, 1151 East Hermans Road, Tucson, AZ 85756, USA*

⁷*University of Vienna, Dept. of Astrophysics, Turken-schanzstraße 17, A-1180 Wien, Austria*

Abstract. The evolution and lifetimes of thermally pulsating asymptotic giant branch (TP-AGB) stars suffer from significant uncertainties. We present a detailed framework for constraining model luminosity functions of TP-AGB stars using resolved stellar populations. We show an example of this method that compares various TP-AGB mass-loss prescriptions that differ in their treatments of mass loss before the onset of dust-driven winds (pre-dust). We find that models with more efficient pre-dust driven mass loss produce results consistent with observations, as opposed to more canonical mass-loss models. Efficient pre-dust driven mass-loss predicts for $[\text{Fe}/\text{H}] \lesssim -1.2$, lower mass TP-AGB stars ($M \lesssim 1M_{\odot}$) must have lifetimes less than about 1.2 Myr.

1. Introduction

Resolved stellar populations (RSPs) are powerful laboratories for understanding uncertain phases of stellar evolution, including the thermally pulsating asymptotic giant branch (TP-AGB; e.g., Marigo et al. 2008). Understanding TP-AGB stars in dwarf galaxies shed light on the processes of galaxies at larger redshift where resolving the stellar content is impossible. In addition, TP-AGB stars can also contribute $\sim 20\%$ of a galaxy's NIR light (Melbourne et al. 2012).

Despite their importance, TP-AGB models uncertainly predict the brightness distribution (i.e., the luminosity function; LF) of AGB stars beyond the MCs (e.g., see discussion in Girardi et al. 2010). The differences between observed and modeled LFs

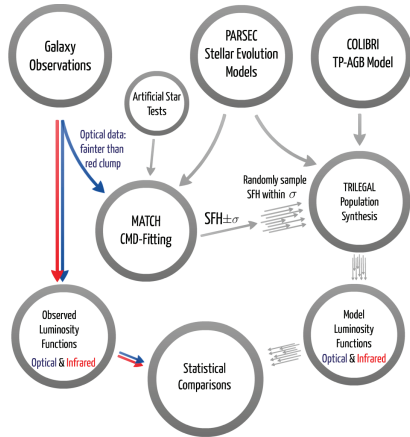


Figure 1. Schematic diagram of the method to statistically compare the predicted TP-AGB model luminosity function to that observed (see text).

of TP-AGB stars found in a RSP is mainly due to model TP-AGB lifetimes, which are primarily set by mass loss (e.g., Vassiliadis & Wood 1993).

Recently, the Hubble Space Telescope has optically imaged ~ 70 nearby galaxies that together house thousands of TP-AGB stars (Dalcanton et al. 2009). From this sample, 23 galaxies also have HST/NIR imaging (Dalcanton et al. 2012). These datasets provide over 1000, low metallicity, TP-AGB stars which we use to constrain model TP-AGB mass-loss prescriptions, and thus TP-AGB model lifetimes. Here, we outline a method expanded from Girardi et al. (2010) to constrain uncertain parameters of TP-AGB models with observations of RSPs, and illustrate the method with summary analysis presented in Rosenfield et al. (2014). By ensuring a large model parameter search space, this method is a step toward the goal of a fully Bayesian framework for constraining stellar evolution models.

2. Method

Fig. 1 is a schematic diagram of the method to statistically compare TP-AGB models with observations. We are primarily interested the shape of the LF brighter than the tip of the red giant branch (TRGB). However, this method is applicable to higher dimensional data, such as color-magnitude diagrams (CMDs) and color-color diagrams of any RSP. Briefly, we compare the observed LFs to synthetic RSPs that are created based on the most likely star formation history (SFH) of the data and a specified TP-AGB mass-loss prescription.

2.1. Observed Luminosity Functions

Beginning in the top left of Fig. 1, luminosity functions are obtained from the optical and NIR data. Using the optical data, we also calculate at least 100,000 artificial star tests for each image (described in e.g., Dalcanton et al. 2009), which are used to establish a faint magnitude limit (set at 90% completeness) to compare LFs, are applied to the stellar evolution models when deriving the SFH, and applied to the model LFs to

correct for completeness. In addition, RGB stars are counted in order to scale the population synthesis models that provide the model LFs (RGB stars are usually identified by a CMD box, c.f., Girardi et al. 2010; Rosenfield et al. 2014; Melbourne et al. 2012).

2.2. Model Luminosity Functions

2.2.1. Stellar Evolution Models

Two stellar evolution codes are used in recovering the SFH of the galaxy and to create synthetic stellar populations (top and right of Fig. 1).

Padova and Trieste Stellar Evolution Code: PARSEC v1.1 (Bressan et al. 2012) is an updated Padova Stellar Evolution code, containing models spanning $Z = 0.0001 - 0.06$, $M = 0.1 - 12M_{\odot}$, from the Pre-MS to either the TP-AGB or core Carbon ignition.

COLIBRI: Following the first thermal pulse on the AGB, COLIBRI takes over the stellar evolution calculations from PARSEC (Marigo et al. 2013). Briefly, COLIBRI optimizes the ratio of physical accuracy over computational issues typical of TP-AGB models, counting on a detailed envelope model in which the molecular chemistry of >800 species and gas opacities are computed on-the-fly (Marigo & Aringer 2009).

2.2.2. Star Formation Histories

SFHs are derived using the CMD-fitting MATCH package (Dolphin 2000) using the deeper optical data. MATCH finds the most-likely CMD that fits the optical CMD based on a given IMF, binary fraction, artificial star tests, and stellar models. In this work, we adopt a Kroupa (2001) IMF and a binary fraction of 0.35.

The input stellar models used in MATCH are from PARSEC, that is, we exclude TP-AGB models in the SFH derivation and give no weight to the regions of the observed CMD above the measured TRGB and redder than the main sequence.

Uncertainties in the SFHs propagate to a spread in the predicted LF (see Fig. 2). We use the most-likely SFH and its random uncertainties as inputs to the population synthesis models (for complete details see Dolphin 2013).

2.2.3. Population Synthesis

We model the photometry of RSPs with the TRILEGAL population synthesis code (Girardi et al. 2005). TRILEGAL takes as input the PARSEC and COLIBRI stellar evolution models, an IMF, binary fraction, and the time evolution of metallicity and star formation rate. Importantly, TRILEGAL also simulates the $L - T_{\text{eff}}$ variations due to the thermal pulse cycles on the TP-AGB (Girardi & Marigo 2007). The TRILEGAL input parameters are set to remain consistent with the parameters listed in Sec. 2.2.2. Finally, to fully explore the possible parameter space, we randomly draw SFHs from the most-likely SFH and its given uncertainties.

Each synthetic RSP is scaled to match the number of RGB stars identified from the observations. The scaled luminosity functions are finally corrected for completeness based on the artificial star tests.

2.3. Statistical Comparisons

The resulting set of model and observed LFs are compared by using a statistic similar to χ^2 but for a Poisson probability distribution (e.g., Dolphin 2002).

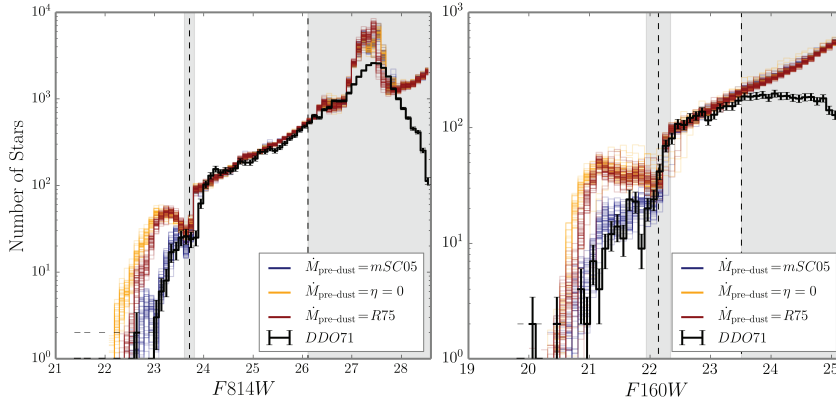


Figure 2. LFs of DDO71 with three mass loss prescriptions $\eta = 0$, $R75$, and $mSC05$. The spread in model LFs is due to sampling the most-likely SFH and its uncertainties. The faintest shaded region marks the 90% completeness limit, and brighter shaded region denotes the TRGB (Dalcanton et al. 2009, 2012).

3. Comparing Three Mass Loss Prescriptions

As an example of the success of this method we summarize recent findings from Rosenfield et al. (2014) which emphasized the importance of mass loss on the AGB before the onset of dust-driven winds. In this work, we compared the results of this method using three pre-dust mass loss regimes: 1) no pre-dust mass loss ($\eta = 0$); 2) The canonical (Reimers 1975, $R75$) mass-loss with efficiency $\eta = 0.4$; and 3) a modified version of (Schröder & Cuntz 2005) based on (Cranmer & Saar 2011, $mSC05$). Fig. 2 shows the model LFs with each mass loss prescription as a visual guide. Clearly, ignoring pre-dust mass loss or simply using $R75$ over-predicts the number of TP-AGB stars, and $mSC05$ is a promising fit. In terms of the Poisson likelihood parameter, $mSC05$ is a factor of 2-3 lower than the other prescriptions. Using $mSC05$, we show the resulting lifetimes of TP-AGB stars as a function of mass for a range of metallicities in Fig. 3.

4. Conclusions

We have presented a framework for constraining stellar evolution models and showed its use in constraining low mass, low metallicity, TP-AGB mass-loss rates, which emphasizes the importance of including efficient pre-dust mass loss in TP-AGB models. Specifically, $mSC05$ predicts for $[\text{Fe}/\text{H}] \lesssim -1.2$, lower mass TP-AGB stars ($M \lesssim 1M_{\odot}$) must have lifetimes less than about 1.2 Myr.

Acknowledgments. Based on observations made with the NASA/ESA Hubble Space Telescope, obtained from the Data Archive at the Space Telescope Science Institute (STScI), which is operated by the Association of Universities for Research in Astronomy, Inc., under NASA contract NAS 5-26555. We acknowledge support from Progetto di Ateneo 2012 (University of Padova, ID: CPDA125588/12), HST GO-10915, and the ERC Consolidator Grant (ID: 610654, project STARKEY). Support for DRW is from NASA through Hubble Fellowship grants HST-HF-51331.01 awarded by the STScI.

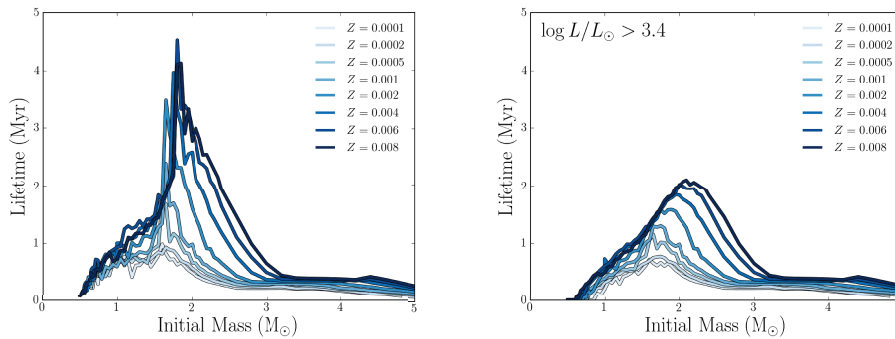


Figure 3. Lifetime of TP-AGB stars as a function of initial mass for several metallicities predicted by the *mSC05* model. Left: the total lifetime of the pre-dust phase. Right: the lifetime of the TP-AGB phase brighter than the TRGB (measurable from observations).

References

- Bressan, A., Marigo, P., Girardi, L., Salasnich, B., Dal Cero, C., Rubele, S., & Nanni, A. 2012, *MNRAS*, 427, 127
- Cranmer, S. R., & Saar, S. H. 2011, *ApJ*, 741, 54
- Dalcanton, J. J., Williams, B. F., Melbourne, J. L., Girardi, L., Dolphin, A., Rosenfield, P. A., Boyer, M. L., de Jong, R. S., Gilbert, K., Marigo, P., Olsen, K., Seth, A. C., & Skillman, E. 2012, *ApJS*, 198, 6
- Dalcanton, J. J., Williams, B. F., Seth, A. C., Dolphin, A., Holtzman, J., Rosema, K., Skillman, E. D., Cole, A., Girardi, L., Gogarten, S. M., Karachentsev, I. D., Olsen, K., Weisz, D., Christensen, C., Freeman, K., Gilbert, K., Gallart, C., Harris, J., Hodge, P., de Jong, R. S., Karachentseva, V., Mateo, M., Stetson, P. B., Tavarez, M., Zaritsky, D., Governato, F., & Quinn, T. 2009, *ApJS*, 183, 67
- Dolphin, A. E. 2000, *PASP*, 112, 1383
- 2002, *MNRAS*, 332, 91
- 2013, *ApJ*, 775, 76
- Girardi, L., Groenewegen, M. A. T., Hatziminaoglou, E., & da Costa, L. 2005, *A&A*, 436, 895
- Girardi, L., & Marigo, P. 2007, *A&A*, 462, 237
- Girardi, L., Williams, B. F., Gilbert, K. M., Rosenfield, P., Dalcanton, J. J., Marigo, P., Boyer, M. L., Dolphin, A., Weisz, D. R., Melbourne, J., Olsen, K. A. G., Seth, A. C., & Skillman, E. 2010, *ApJ*, 724, 1030
- Kroupa, P. 2001, *MNRAS*, 322, 231
- Marigo, P., & Aringer, B. 2009, *A&A*, 508, 1539
- Marigo, P., Bressan, A., Nanni, A., Girardi, L., & Pumo, M. L. 2013, *MNRAS*, 434, 488
- Marigo, P., Girardi, L., Bressan, A., Groenewegen, M. A. T., Silva, L., & Granato, G. L. 2008, *A&A*, 482, 883
- Melbourne, J., Williams, B. F., Dalcanton, J. J., Rosenfield, P., Girardi, L., Marigo, P., Weisz, D., Dolphin, A., Boyer, M. L., Olsen, K., Skillman, E., & Seth, A. C. 2012, *ApJ*, 748, 47
- Reimers, D. 1975, *Memoires of the Societe Royale des Sciences de Liege*, 8, 369
- Rosenfield, P., Marigo, P., Girardi, L., Dalcanton, J. J., Bressan, A., Gullieuszik, M., Weisz, D., Williams, B. F., Dolphin, A., & Aringer, B. 2014, *ApJ*, 790, 22
- Schröder, K.-P., & Cuntz, M. 2005, *ApJ*, 630, L73
- Vassiliadis, E., & Wood, P. R. 1993, *ApJ*, 413, 641